

# Linewidth measurement of external grating cavity quantum cascade laser using saturation spectroscopy

Cite as: Appl. Phys. Lett. **92**, 111116 (2008); <https://doi.org/10.1063/1.2901038>

Submitted: 18 February 2008 . Accepted: 03 March 2008 . Published Online: 21 March 2008

Nandini Mukherjee, Rowel Go, and C. Kumar N. Patel



View Online



Export Citation

## ARTICLES YOU MAY BE INTERESTED IN

[Linewidth measurement of mid infrared quantum cascade laser by optical feedback interferometry](#)

Applied Physics Letters **108**, 031105 (2016); <https://doi.org/10.1063/1.4940116>

[Direct and wavelength modulation spectroscopy using a cw external cavity quantum cascade laser](#)

Applied Physics Letters **94**, 201110 (2009); <https://doi.org/10.1063/1.3141521>

[External cavity quantum cascade laser tunable from 7.6 to 11.4  \$\mu\text{m}\$](#)

Applied Physics Letters **95**, 061103 (2009); <https://doi.org/10.1063/1.3193539>

Lock-in Amplifiers  
up to 600 MHz



# Linewidth measurement of external grating cavity quantum cascade laser using saturation spectroscopy

Nandini Mukherjee,<sup>1</sup> Rowel Go,<sup>2</sup> and C. Kumar N. Patel<sup>1,2,a)</sup>

<sup>1</sup>Department of Physics and Astronomy, University of California, Los Angeles, California 90095, USA

<sup>2</sup>Pranalytica, Inc., 1101 Colorado Avenue, Santa Monica, California 90401, USA

(Received 18 February 2008; accepted 3 March 2008; published online 21 March 2008)

A room temperature external grating cavity (EGC) quantum cascade laser (QCL) is characterized using saturation spectroscopy of NO<sub>2</sub>. The presence of two strong EGC QCL waveguide modes is evident from the saturation spectra. A linewidth of 21 MHz for each EGC-QCL mode is measured from the width of the saturation peak at 10 mTorr pressure of NO<sub>2</sub>. © 2008 American Institute of Physics. [DOI: 10.1063/1.2901038]

The development of high power cw room temperature quantum cascade lasers (QCLs) has opened expanded possibilities for high resolution molecular spectroscopy.<sup>1-3</sup> Both the distributed feedback (DFB) and external grating cavity (EGC) QCLs have shown promise in molecular spectroscopy<sup>4</sup> and trace gas detection reaching a detection limit of less than 1 ppb (parts per 10<sup>9</sup>).<sup>5</sup> The DFB QCLs are simpler to use but their tuning range is limited to a few cm<sup>-1</sup>. With a wide tuning range of ~40 cm<sup>-1</sup>, the EGC QCLs are expected to be particularly useful for a broad range of high resolution molecular spectroscopy applications. Molecular lines separated by 0.006 cm<sup>-1</sup> have been resolved using linear spectroscopy with EGC QCL.<sup>6</sup> Although this result indicates an upper limit for the laser linewidth, no direct measurement of the linewidth for an external grating cavity QCL has been reported to date. Here, we report a direct measurement of laser linewidth using sub-Doppler saturation spectroscopy of NO<sub>2</sub> molecules. Although Lamb dip spectroscopy using DFB QCL has been demonstrated,<sup>7,8</sup> EGC QCL has not been employed for saturation spectroscopy of molecules.

The EGC laser consisted of a QCL gain chip (on loan from Pranalytica, Inc.), an aspheric ZnSe lens ( $f/0.7$ ), and a Littrow grating with 240 grooves/mm. The first order diffraction from the Littrow grating provides the necessary feedback for the EGC operation of the QCL. The QCL gain chip has a ridge waveguide structure with a gain length of 4 mm. Electrical and thermal packaging and mounting of the QCL gain chip is described elsewhere.<sup>2</sup> At room temperature, the QCL has its emission peak near 6.3  $\mu$ m. The uncoated facets of the QCL waveguide introduce a loss modulation for the EGC modes. The free spectral range (FSR) of this modulation is ~11 GHz corresponding to a 4 mm length of the QCL. The frequency of the oscillating EGC mode is determined by the convolution of QCL Fabry-Pérot (FP) spectrum (~11 GHz) and the grating reflection spectrum bandwidth ~33 GHz. The EGC length is changed by translating the grating with a piezoactuated positioner (PZT) with 3 nm resolution. With an EGC FSR of ~1.875 GHz corresponding to an external cavity length of 8 cm, we expect a tuning rate of ~0.6 MHz/nm at the laser wavelength of 6.25  $\mu$ m.

A schematic of the saturation spectroscopy set up is shown in Fig. 1. A CaF<sub>2</sub> wedge reflects ~4% of the forward

and the backward beams into two HgCdTe detectors  $D_1$  and  $D_2$ , respectively. The pump beam is focused into a 85 cm long NO<sub>2</sub> gas cell using a 1 m focal length CaF<sub>2</sub> lens. The pump beam, attenuated by the attenuator  $A$ , is retroreflected by a ZnSe wedge  $B2$ . A combination of retroreflection from the ZnSe wedge and double pass through the attenuator provides a probe beam at an intensity of about 1% of the pump beam. NO<sub>2</sub> pressure is kept at 10 mTorr. Transmission of the probe is recorded as the wavelength of the EGC QCL is scanned with PZT at a fixed QCL current. The signals  $D_2$  and  $D_1$  are detected by a lockin amplifier. Multiple scans are digitally averaged and analyzed.

The PZT tuning rate is calibrated using the saturation spectroscopy of NO<sub>2</sub> covering a broader wavelength region.<sup>9</sup> Using these saturation peaks, a PZT tuning rate of 0.078 nm/ $\mu$ m is deduced. This PZT tuning rate is consistent with the 8 cm external cavity length.

Figure 2 shows the probe transmission when the laser is tuned to 6250.9 nm at a QCL operating current of 1013 mA. Two saturation peaks due to the spin doublets  $P_3^\pm(17)$  are seen in Fig. 2. According to HITRAN, these two spin doublets are separated by 100 MHz, which exceeds their Doppler broadening of 87 MHz. The experimental data of Fig. 2 do not match the expected separation of the two peaks. Figure 3 shows the probe transmission when the input pump power is reduced by a factor of 4. At low pump power, the saturation peaks disappear as expected. However, the molecular transitions are still not resolved. The spectral features of Figs. 2 and 3 are qualitatively explained assuming the presence of two transverse laser modes (TM<sub>00</sub> and TM<sub>01</sub>) with a fre-

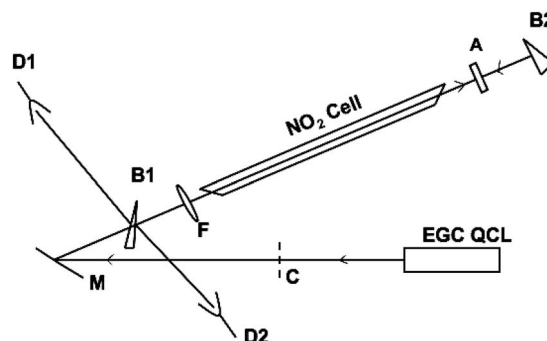


FIG. 1. Schematic of saturation spectroscopy setup ( $M$ : mirror,  $B1$ : CaF<sub>2</sub> wedge,  $B2$ : ZnSe wedge;  $F$ : 1 m focal length lens;  $D1$ ,  $D2$ : HgCdTe detectors;  $C$ : mechanical chopper; and  $A$ : attenuator).

<sup>a)</sup>Electronic mail: patel@physics.ucla.edu.

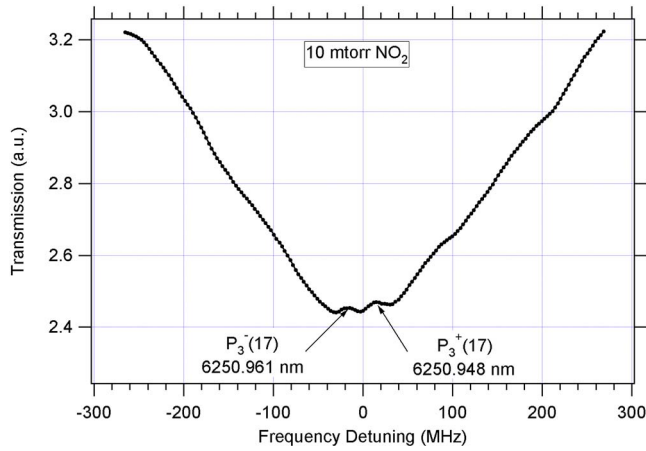


FIG. 2. (Color online) Probe transmission spectra at 6250 nm.

quency separation comparable to the Doppler width. The abnormally wide saturation dips ( $\sim 20$  MHz) in Fig. 2 reflect the effective laser frequency width with sizeable contributions arising from thermal, electrical, and mechanical fluctuations.

With a single mode zero linewidth laser, absorption coefficient of a weak counter propagating probe wave is given by<sup>10</sup>

$$\alpha(\omega) = \alpha_0(\omega) \left\{ 1 - [1 - (1 + G)^{-1/2}] L \left( \frac{(\omega - \omega_0)}{\Gamma} \right) \right\}, \quad (1)$$

where  $\alpha_0$  is the Doppler broadened unsaturated absorption coefficient in absence of the pump,  $G$  is the saturation parameter, and  $L$  is the Lorentzian describing the power broadened homogeneous line shape of the molecular resonance (with  $\Gamma$  being the power broadened homogeneous linewidth). The absorption coefficient is strongly modified in the presence of laser frequency fluctuation. With a Gaussian distribution of laser frequency, we can show that

$$\alpha(\omega) = \alpha_p \left\{ e^{-(\omega - \omega_0/\Delta_D)^2} - \frac{\sqrt{\pi}\Gamma}{\Delta_l} \left[ 1 - \frac{1}{\sqrt{1+G}} \right] e^{-(\omega - \omega_0/\Delta_l)^2} \right\}, \quad (2)$$

where  $\Delta_D$  and  $\Delta_l$  are the Doppler width and laser linewidths, respectively.

In the presence of two laser modes with frequencies  $\omega_1$  and  $\omega_2$ , the transmission of the weak probe beam is given by

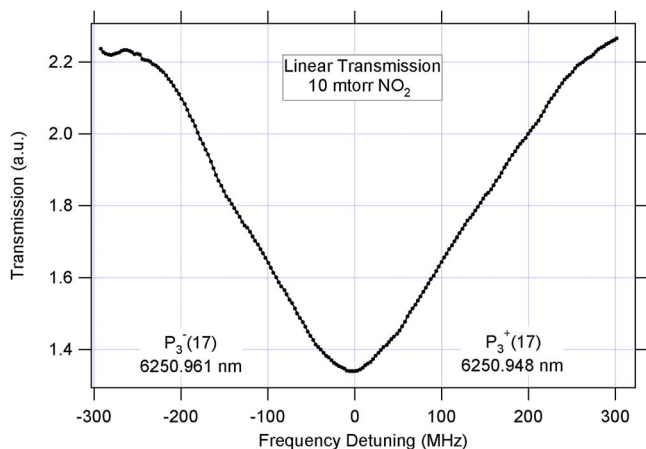


FIG. 3. (Color online) Probe transmission at reduced pump power.

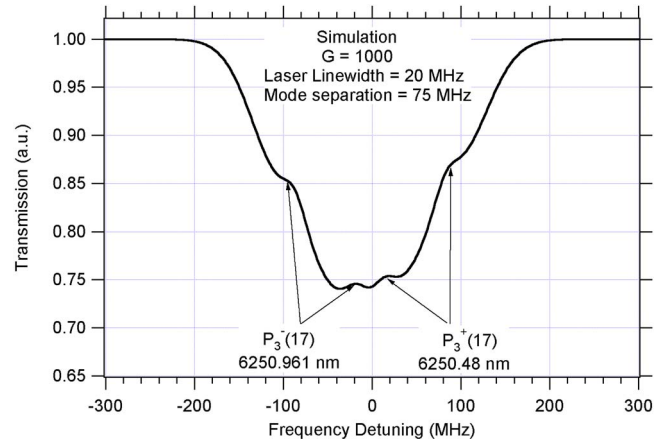


FIG. 4. (Color online) Simulated transmission at 6250 nm.

$$T = \frac{\exp[-\alpha_1(\omega_1 - \omega_0)Z] + r \exp[-\alpha_2(\omega_2 - \omega_0)Z]}{1 + r}, \quad (3)$$

where  $r$  is the intensity ratio of the laser modes,  $Z$  is the path length, and  $\omega_0$  is the molecular resonance frequency.  $\alpha_1$  and  $\alpha_2$  are the saturated absorption coefficients of the laser modes calculated from Eq. (2) using their respective saturation parameters. Results of simulations based on the above model are shown in Figs. 4 and 5. With a laser mode separation  $\omega_1 - \omega_2 = 75$  MHz and a saturation parameter  $G = 1000$ , the simulated spectra qualitatively duplicate the experimental observations of Figs. 2 and 3. The simulation in Fig. 4 shows that the combination of laser frequency fluctuation and presence of two modes dramatically reduces the contrast in saturated transmission (shallower Lamb dips even with large  $G$ ) in agreement with the experimental observation in Fig. 2. The two peaks on the right side of zero detuning in Fig. 4 correspond to the saturation of  $P_3^+(17)$  transition by the two laser modes with a frequency separation of 75 MHz. The conjugate peaks on the left side of the zero detuning are due to repeated saturation of  $P_3^-(17)$  transition. In the experimental spectra of Fig. 2, the shoulder peaks are not fully resolved. The simulated spectra in Fig. 5 at reduced power show that the molecular lines are no longer resolved in the presence of two transverse modes in agreement with the experimental observation in Fig. 3. Although the saturation features in the experiment, Fig. 2, and simulation, Fig. 4, are comparable, the overall width of the transmission spectra

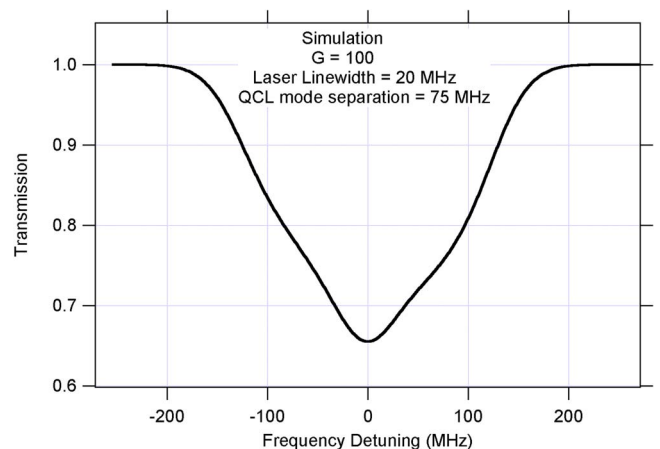


FIG. 5. (Color online) Simulated transmission at reduced pump power.

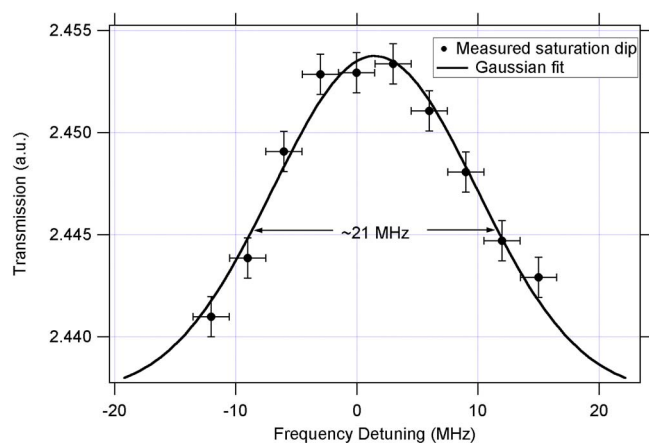


FIG. 6. (Color online) Gaussian fit to the saturation dip at 6250.961 nm.

does not match. At present, we have no reasonable explanation.

We estimate the transition dipole moment using the saturation parameter  $G=1000$  required to simulate the experimental spectra. The transition dipole moment is found from the saturation intensity  $I_s = \epsilon_0 c \hbar^2 \gamma^2 / 2 \mu^2$ . The transverse relaxation  $\gamma = \pi(\Delta\nu_p + \Delta\nu_{tr})$ , where  $\Delta\nu_p$  and  $\Delta\nu_{tr}$  are the collisional and the transit time broadening, respectively. Using the self-broadening parameter of Ref. 11, we estimate  $\Delta\nu_p \approx 80$  KHz. Following Refs. 12 and 13, with a 2 mm Gaussian beam, we calculate  $\Delta\nu_{tr} \approx 82$  KHz for  $\text{NO}_2$  at room temperature. With  $G=1000$  and a laser mode power of  $P=18$  mW, we find  $\mu \approx 0.24$  D for the  $P_3^\pm(17)$  transition. This transition dipole moment compares well with 0.21 D from HITRAN.

One of the saturation peaks of Fig. 2 is shown enlarged in Fig. 6. In the presence of small collisional and transit time broadening ( $\sim 100$  KHz), the width of the saturation peak reflects the linewidth of an EGC QCL mode. A linewidth of 21 MHz ( $0.0007 \text{ cm}^{-1}$ ) for an EGC QCL mode is estimated from the Gaussian fit of the saturation peak in Fig. 6. A comparison between a Lorentzian and a Gaussian fit shows that the saturation peak fits better with a Gaussian. The observed linewidth originates from the QCL frequency fluctuations arising from residual electrical, thermal, and mechani-

cal noise and does not reflect the intrinsic linewidth of an EGC QCL.

In conclusion, saturation spectroscopy of  $\text{NO}_2$  at 10 mTorr pressure is utilized to characterize an EGC QCL near  $6 \mu\text{m}$  wavelength. Using Lamb dips in transmission, 21 MHz laser linewidth is measured for an EGC QCL mode and laser wavelength is calibrated to within the accuracy of the laser linewidth. Our experiment shows that a well calibrated EGC QCL mode has sufficient power for nonlinear spectroscopy and it has narrow linewidth to address individual molecular lines and extract molecular parameters such as molecular dipole moments. A Gaussian fitting to the saturation peak suggests that the presently observed laser linewidth is due to frequency fluctuation, which can be improved by passive and active frequency stabilizations.

This work (for Go and Patel) was partially supported through an ATP Grant No. 70NANB3H3026.

- <sup>1</sup>G. Wysocki, A. A. Kosterev, and F. K. Tittel, *Appl. Phys. B: Lasers Opt.* **4-5**, 617 (2005).
- <sup>2</sup>A. Tsekoun, R. Go, M. Pushkarsky, M. Razeghi, and C. K. N. Patel, *Proc. Natl. Acad. Sci. U.S.A.* **103**, 4831 (2006).
- <sup>3</sup>J. S. Yu, S. Slivken, A. Evans, L. Doris, and M. Razeghi, *Appl. Phys. Lett.* **83**, 2503 (2003).
- <sup>4</sup>D. Weidmann, F. K. Tittel, T. Aellen, M. Beck, D. Hofstetter, J. Faist, and S. Blaser, *Appl. Phys. B: Lasers Opt.* **79**, 907 (2004).
- <sup>5</sup>M. Pushkarsky, A. Tsekoun, I. G. Dunayevskiy, R. Go, and C. K. Patel, *Proc. Natl. Acad. Sci. U.S.A.* **103**, 10846 (2006).
- <sup>6</sup>G. Wysocky, R. F. Curl, F. K. Tittel, R. Maulini, J. M. Bulliard, and J. Faist, *Appl. Phys. B: Lasers Opt.* **81**, 769 (2005).
- <sup>7</sup>J. T. Remillard, D. Uy, W. H. Weber, F. Capaso, C. Gamchl, A. L. Hutchinson, D. L. Sivco, J. N. Baillargeon, and A. Y. Cho, *Opt. Express* **7**, 243 (2000).
- <sup>8</sup>A. S. Castrillo, E. De Tommasi, L. Gianfrani, L. Sirigu, and J. Faist, *Opt. Lett.* **31**, 3040 (2006).
- <sup>9</sup>N. Mukherjee and C. K. N. Patel (unpublished).
- <sup>10</sup>V. S. Letokov, in *High Resolution Laser Spectroscopy*, edited by K. Shimoda (Springer, Berlin 1976), pp. 96–171.
- <sup>11</sup>V. Malathy Devi, B. Fridovich, G. D. Jones, D. G. S. Snyder, Palash P. Das, J.-M. Flaud, C. Camy-Peyret, and K. Narahari Rao, *J. Mol. Spectrosc.* **93**, 179 (1982).
- <sup>12</sup>C. J. Borde, J. L. Hall, C. V. Kunasz, and D. G. Hummer, *Phys. Rev. A* **14**, 236 (1976).
- <sup>13</sup>V. S. Letokhov and V. P. Chebotayev, *Nonlinear Laser Spectroscopy* (Springer, Berlin, 1977).